



OPEEPEESWAY LAKE AREA

Ontario Airborne Geophysical Surveys Magnetic, Electromagnetic and Radiometric Data Geophysical Data Set 1238

Ontario Geological Survey
Ministry of Northern Development and Mines
Willet Green Miller Centre
933 Ramsey Lake Road
Sudbury, Ontario, P3E 6B5
Canada

TABLE OF CONTENTS

CREDITS.....	2
DISCLAIMER.....	2
CITATION	2
1. INTRODUCTION.....	3
2. SURVEY LOCATION AND SPECIFICATIONS.....	4
3. AIRCRAFT, PERSONNEL AND EQUIPMENT.....	5
4. CONTRACTOR DATA PROCESSING	11
5. FINAL DATA COMPILATION AND PROCESSING.....	20
6. FINAL PRODUCTS.....	25
REFERENCES.....	27
APPENDIX A GENERAL ARCHIVE DEFINITION.....	28
APPENDIX B PROFILE ARCHIVE DEFINITION.....	31
APPENDIX C ANOMALY ARCHIVE DEFINITION	33
APPENDIX D KEATING CORRELATION ARCHIVE DEFINITION	34
APPENDIX E GRID ARCHIVE DEFINITION.....	35
APPENDIX F GEOTIFF AND VECTOR ARCHIVE DEFINITION.....	36

CREDITS

List of accountabilities and responsibilities:

- Jack Parker, Senior Manager, Precambrian Geoscience Section, Ontario Geological Survey (OGS), Ministry of Northern Development and Mines (MNDM) – accountable for the airborne geophysical survey projects, including contract management
- Steve Munro, Senior Geophysicist, Scott Hogg & Associates Ltd. (SHA), Toronto, Ontario, responsible for the reprocessing of this data set
- Tom Watkins, Team Leader, Publication Services Section, Ontario Geological Survey, MNDM – managed the project-related hard copy products
- Desmond Rainsford, Geophysicist, Precambrian Geoscience Section, Ontario Geological Survey, MNDM – managed the project-related digital products
- Fugro Airborne Surveys Corp., Mississauga – data acquisition and data compilation.

DISCLAIMER

To enable the rapid dissemination of information, this digital data has not received a technical edit. Every possible effort has been made to ensure the accuracy of the information provided; however, the Ontario Ministry of Northern Development and Mines does not assume any liability or responsibility for errors that may occur. Users may wish to verify critical information.

CITATION

Information from this publication may be quoted if credit is given. It is recommended that reference be made in the following form:

Ontario Geological Survey 2012. Ontario airborne geophysical surveys, magnetic, electromagnetic and radiometric data, Opepeesway Lake area—Purchased data; Ontario Geological Survey, Geophysical Data Set 1238.

Users of OGS products are encouraged to contact those Aboriginal communities whose traditional territories may be located in the mineral exploration area to discuss their project.

1. INTRODUCTION

As part of an ongoing program to acquire high-quality, high-resolution airborne geophysical data across the Province of Ontario, the Ontario Ministry of Northern Development and Mines (MNDM) does, from time to time, issue Requests For Data (RFD) in order to purchase existing proprietary data held by mining companies. Purchase of existing data complements new surveys commissioned by the MNDM.

The purchase of data is attractive because of the low cost of acquisition relative to flying new surveys.

The money used to purchase the data can be reinvested in exploration. The data are assessed for quality prior to purchase and are reprocessed to meet the common formats and standards of other Ontario geophysical data. Once reprocessed these data are then made public.

Ranking and valuation of submitted airborne geophysical survey data sets were based on the following criteria:

- date of survey – recent surveys were favoured over older surveys because of improved acquisition technology, greater data density and improved final products.
- survey method – magnetometer surveys, without supplementary radiometrics or very low frequency (VLF), were given the lowest rating in this category; airborne electromagnetic (AEM) and magnetometer were given the highest; the objective was to acquire data that complements what is already available in the public domain, with emphasis on exploration rather than mapping.
- location of area
 - data sets occurring within areas already surveyed or scheduled for survey were selected only if they added significantly to the acquired data sets,
 - proximity or coincidence of the survey block with areas having restricted land use designations affected the value assigned to that survey,
 - consideration was given to data sets that were collected in remote areas where logistical costs are very high.
- line spacing – detailed surveys were normally accorded a higher rating than reconnaissance surveys.
- quality of data – data quality, processed products, and adherence to correct survey specifications had to be up to normal industry standards.
- survey size – data sets comprising less than 1000 line-km were selected only if they fell in very strategic locations.
- other criteria – factors such as apparent mineral significance, previous exploration activity and land availability were also considered in making the final selection.

2. SURVEY LOCATION AND SPECIFICATIONS

This report describes a helicopter-borne DIGHEM electromagnetic, magnetic and gamma spectrometer survey located approximately 140 km northwest of Sudbury, Ontario. The survey was flown on behalf of Augen Gold Corp. and was conducted by Fugro Airborne Surveys Corp., Ontario (Fugro 2008). The survey was completed on November 10, 2007.

The survey was flown with a 45° to 225° line direction with 150 m, 75 m and 37.5 m line spacing. Total survey coverage was 3035 line-km. The map below (Figure 1) shows the location of the survey area.

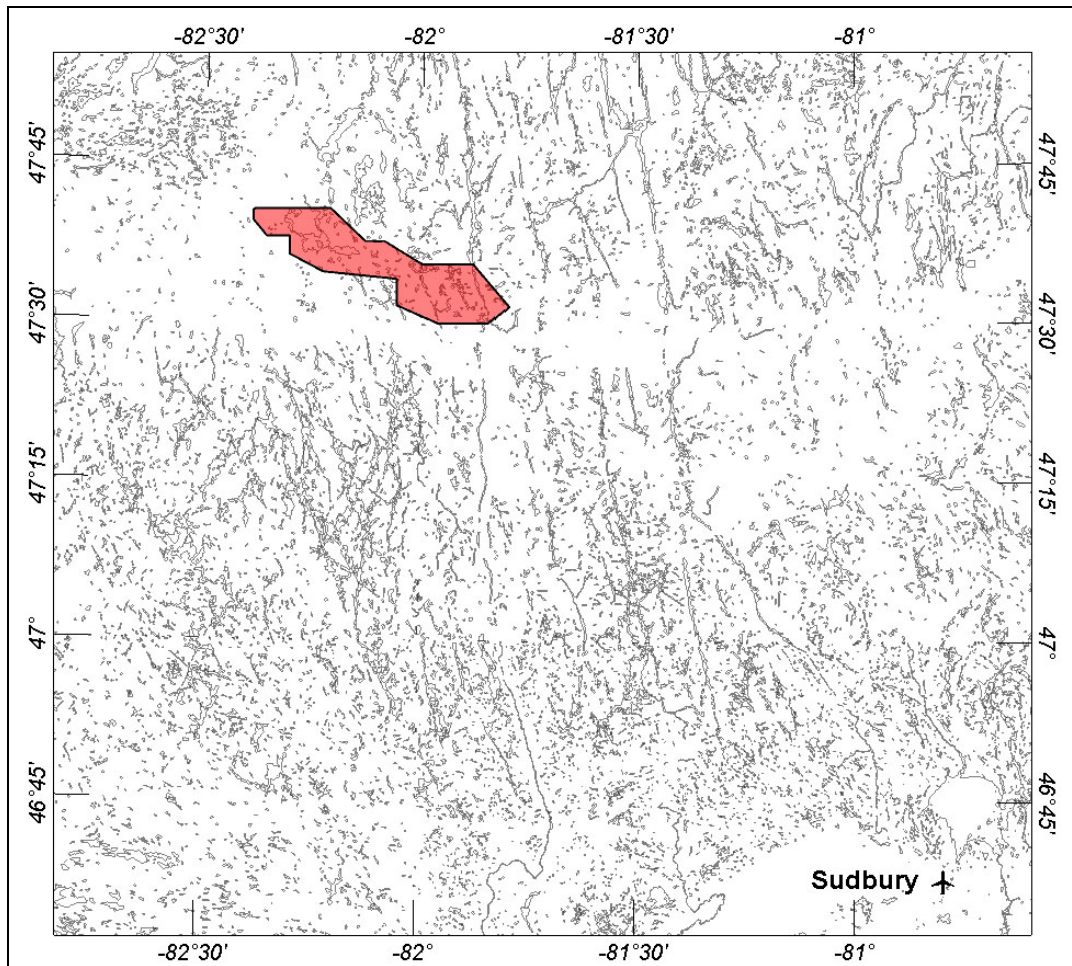


Figure 1 – Survey Index Map

The table below summarizes the flight specifications

Parameter	Specifications
Traverse line direction	045°/225°
Traverse line spacing	150 m; 75 m; 37.5 m
Tie line direction	135°/315°
Tie line spacing	1500 m
Sample interval	10 Hz, 3.3 m @ 120 km/h
Aircraft mean terrain clearance	58 m
EM sensor mean terrain clearance	30 m
Mag. sensor mean terrain clearance	30 m
Spectrometer crystal package (on helicopter)	58 m
Average speed	120 km/h
Navigation (guidance)	±5 m, Real-time GPS
Post-survey flight path	±2 m, Differential GPS

3. AIRCRAFT, PERSONNEL AND EQUIPMENT

Aircraft

The survey was carried out using an AS350-B2 helicopter, owned and operated by Questral Helicopters Ltd.

Personnel

The following personnel were involved in the acquisition, processing and interpretation of the data.

David Miles	Manager, Helicopter Operations
Emily Farquhar	Manager, Data Processing and Interpretation
Parag Paliwal	Geophysical Operator (Oct. 7 to Nov. 11)
Sunny Bhatia	Geophysical Operator (Oct. 7 to 29)
Laura Quigley	Field Geophysicist/Crew Leader (Oct. 7 to 30)
Dima Amine	Field Geophysicist/Crew Leader (Nov. 1 to 11)
David Lu	Field Data Processor (Oct. 30 to Nov. 11)
Stephen Harrison	Geophysicist/ Data Processor
Paul A. Smith	Interpretation Geophysicist
Lyn Vanderstarren	Drafting Supervisor
Susan Pothiah	Word Processing Operator
Albina Tonello	Secretary/Expeditior
Matt Richie	Pilot (Questral Helicopters Ltd.)

Electromagnetic System

Model: DIGHEM^V – BKS50

Type: Towed bird, symmetric dipole configuration operated at a nominal survey altitude of 30 m. Coil separation is 8 m for 900 Hz, 1000 Hz, 5500 Hz and 7200 Hz, and 6.3 m for the 56 000 Hz coil pair.

Coil orientations, frequencies and dipole moments

Moment (Atm ²)	Coil Orientation	Nominal frequency	Actual frequency
211	coaxial	1000 Hz	1120 Hz
211	coplanar	900 Hz	910 Hz
67	coaxial	5500 Hz	5450 Hz
56	coplanar	7200 Hz	7110 Hz
15	coplanar	56 000 Hz	55 800 Hz

Channels recorded

5 in-phase channels
5 quadrature channels
2 monitor channels

Sensitivity

0.06 ppm at 1000 Hz Coaxial
0.12 ppm at 900 Hz Coplanar
0.12 ppm at 5500 Hz Coaxial
0.24 ppm at 7200 Hz Coplanar
0.60 ppm at 56 000 Hz Coplanar

Sample rate

10 per second, equivalent to 1 sample every 3.3 m, at a survey speed of 120 km/h.

The electromagnetic system utilizes a multi-coil coaxial/coplanar technique to energize conductors in different directions. The coaxial coils are vertical with their axes in the flight direction. The coplanar coils are horizontal. The secondary fields are sensed simultaneously by means of receiver coils that are maximum-coupled to their respective transmitter coils. The system yields an in-phase and a quadrature channel from each transmitter-receiver coil-pair.

In-Flight EM System Calibration

Calibration of the system during the survey uses the Fugro AutoCal automatic, internal calibration process. At the beginning and end of each flight, and at intervals during the flight, the system is flown up to high altitude to remove it from any “ground effect” (response from the earth). Any remaining signal from the receiver coils (base level) is measured as the zero level,

and is removed from the data collected until the time of the next calibration. Following the zero level setting, internal calibration coils, for which the response phase and amplitude have been determined at the factory, are automatically triggered – one for each frequency. The on-time of the coils is sufficient to determine an accurate response through any ambient noise. The receiver response to each calibration coil “event” is compared to the expected response (from the factory calibration) for both phase angle and amplitude, and any phase and gain corrections are automatically applied to bring the data to the correct value.

In addition, the outputs of the transmitter coils are continuously monitored during the survey, and the gains are adjusted to correct for any change in transmitter output.

Because the internal calibration coils are calibrated at the factory (on a resistive half space) ground calibrations using external calibration coils onsite are not necessary for system calibration. A check calibration may be carried out onsite to ensure all systems are working correctly. All system calibrations will be carried out in the air, at sufficient altitude that there will be no measurable response from the ground.

The internal calibration coils are rigidly positioned and mounted in the system relative to the transmitter and receiver coils. In addition, when the internal calibration coils are calibrated at the factory, a rigid jig is employed to ensure accurate response from the external coils.

Using real-time Fast Fourier Transforms and the calibration procedures outlined above, the data are processed in real time, from measured total field at a high sampling rate, to in-phase and quadrature values at 10 samples per second.

Airborne Magnetometer

Model: Fugro D1344 processor with Geometrics GR822A sensor
Type: Optically pumped cesium vapour
Sensitivity: 0.01 nT
Sample rate: 10 per second

The magnetometer sensor is housed in the EM bird, 28 m below the helicopter.

Magnetic Base Station

Model: Fugro CF1 base station with timing provided by integrated GPS
Sensor type: Scintrex CS2 (Cesium)
Counter specifications: Accuracy: ± 0.1 nT
Resolution: 0.01 nT
Sample rate 1 Hz

The radar altimeter measures the vertical distance between the helicopter and the ground. This information is used in the processing algorithm that determines conductor depth.

Barometric Pressure and Temperature Sensors

Model: DIGHEM D 1300
Type: Motorola MPX4115AP analog pressure sensor AD592AN high-Impedance remote temperature sensors
Sensitivity: Pressure: 150 mV/kPa
Temperature: 100 mV/°C or 10 mV/°C (selectable)
Sample rate: 10 per second

The D1300 circuit is used in conjunction with 1 barometric sensor and up to 3 temperature sensors. Two sensors (barometric and temperature) are installed in the EM console in the aircraft, to monitor pressure (KPA) and internal (TEMP_INT) temperature. A third sensor is installed in the bird to monitor external (TEMP_EXT) operating temperatures.

Digital Data Acquisition System

Manufacturer: Fugro
Model: HELIDAS – Integrated Data Acquisition System
Recorder: Compact Flash Card

The stored data are downloaded to the field workstation PC at the survey base, for verification, backup and preparation of in-field products.

Video Flight Path Recording System

Type: Panasonic WVCL322 Colour Video Camera
Recorder: Axis Tablet Computer
Format: .BIN/.BDX

Fiducial numbers are recorded continuously and are displayed on the margin of each image. This procedure ensures accurate correlation of data with respect to visible features on the ground.

Spectrometer

Manufacturer: Exploranium
Model: GR-820. (S.N. 8228)
Type: 256 Multichannel, Thorium stabilized
Accuracy: 1 count/sec.
Update: 1 integrated sample/sec.

The GR-820 Airborne Spectrometer employs 4 downward looking crystals (1024 cu.in. 6.8 L) and one upward looking crystal (256 cu.in.- 4.2 L). The downward crystal records the radiometric spectrum from 410 KeV to 3 MeV over 256 discrete energy windows, as well as a cosmic ray channel which detects photons with energy levels above 3.0 MeV. From these 256

channels, the standard Total Count, Potassium, Uranium and Thorium channels are extracted. The upward crystal is used to measure and correct for Radon. The shock-protected Sodium Iodide (Thallium) crystal package is unheated, and is automatically stabilized with respect to the Thorium peak. The GR-820 provides raw or Compton stripped data that has been automatically corrected for gain, base level, ADC offset and dead time. The system is calibrated before and after each flight using three accurately positioned hand-held sources. Additionally, fixed-site hover tests or repeat test lines are flown to determine if there are any differences in background. This procedure allows corrections to be applied to each survey flight, to eliminate any differences that might result from changes in temperature or humidity.

4. CONTRACTOR DATA PROCESSING

Quality Control And In-Field Processing

Digital data for each flight were transferred to the field workstation, in order to verify data quality and completeness. A database was created and updated using Geosoft® Oasis Montaj™ and proprietary Fugro Atlas software. This allowed the field personnel to calculate, display and verify both the positional (flight path) and geophysical data on a screen or printer. Records were examined as a preliminary assessment of the data acquired for each flight.

In-field processing of Fugro survey data consists of differential corrections to the airborne GPS data, verification of EM calibrations, drift correction of the raw airborne EM data, spike rejection of all geophysical and ancillary data, verification of flight videos, calculation of preliminary resistivity data, diurnal correction, and preliminary levelling of magnetic data.

All data, including base station records, were checked on a daily basis, to ensure compliance with the survey contract specifications. Re-flights were required if any of the following specifications were not met.

Navigation	Positional (x,y) accuracy of better than 10 m, with a CEP (circular error of probability) of 95%.
Flight Path	No lines to exceed $\pm 25\%$ departure from nominal line spacing over a continuous distance of more than 1 km, except for reasons of safety.
Clearance	Mean terrain sensor clearance of 30 m, ± 10 m, except where precluded by safety considerations, e.g., restricted or populated areas, severe topography, obstructions, tree canopy, aerodynamic limitations, etc.
Airborne Mag.	Non-normalized 4th difference noise envelope not to exceed 1.6 Nt over a distance of more than 1 km.
Base Mag.	Diurnal variations not to exceed 10 nT over a straight line time chord of 1 minute.
EM	Spheric pulses may occur having strong peaks but narrow widths. The EM data area considered acceptable when their occurrence is less than 10 spheric events exceeding the stated noise specification for a given frequency per 100 samples continuously over a distance of 2000 m.

Flight Path Recovery

The raw range data from at least four satellites were simultaneously recorded by both the base and mobile GPS units. The geographic positions of both units, relative to the model ellipsoid, were calculated from this information. Differential corrections, which were obtained from the base station, were applied to the mobile unit data to provide a post-flight track of the aircraft, accurate to within 2 m. Speed checks of the flight path were also carried out to determine if there were any spikes or gaps in the data.

The corrected WGS84 latitude/longitude co-ordinates were transformed to the co-ordinate system used on the final maps. Images or plots were then created to provide a visual check of the flight path.

Electromagnetic Data

EM data were processed at the recorded sample rate of 10 samples/second. Spheric rejection median and Hanning filters were then applied to reduce noise to acceptable levels. EM test profiles were then created to allow the interpreter to select the most appropriate EM anomaly picking controls for a given survey area. The EM picking parameters depend on several factors but are primarily based on the dynamic range of the resistivities within the survey area, and the types and expected geophysical responses of the targets being sought.

Anomalous electromagnetic responses were selected and analysed by computer to provide a preliminary electromagnetic anomaly map. The automatic selection algorithm is intentionally oversensitive to assure that no meaningful responses were missed. Using the preliminary map in conjunction with the multi-parameter stacked profiles, the interpreter then classified the anomalies according to their source and eliminated those that are not substantiated by the data. The final interpreted EM anomaly map included bedrock, surficial and cultural conductors. A map containing only bedrock conductors can be generated, if desired.

The tables below summarize the anomaly statistics.

Conductor Grade	Conductance Range Siemens (mhos)	Number of Responses
7	>100	3
6	50 – 100	2
5	20 – 50	7
4	10 – 20	27
3	5 – 10	58
2	1 – 5	327
1	<1	1352
*	Indeterminate	803
	Total	2579

Conductor Model	Most Likely Source	Number of Responses
L	Line source (culture)	55
D	Discrete bedrock conductor	296
B	Discrete bedrock conductor	174
S	Conductive cover	1834
H	Rock unit or thick cover	1
E	Edge of wide conductor	219
Total		2579

Apparent Resistivity

The apparent resistivities in ohm-m were generated from the in-phase and quadrature EM components for all of the coplanar frequencies, using a pseudo-layer half-space model. The inputs to the resistivity algorithm were the in-phase and quadrature amplitudes of the secondary field. The algorithm calculates the apparent resistivity in ohm-m, and the apparent height of the bird above the conductive source. Any difference between the apparent height and the true height, as measured by the radar altimeter, is called the pseudo-layer and reflects the difference between the real geology and a homogeneous half-space. This difference is often attributed to the presence of a highly resistive upper layer. Any errors in the altimeter reading, caused by heavy tree cover, are included in the pseudo-layer and do not affect the resistivity calculation. The apparent depth estimates, however, will reflect the altimeter errors. Apparent resistivities calculated in this manner may differ from those calculated using other models.

In areas where the effects of magnetic permeability or dielectric permittivity have suppressed the in-phase responses, the calculated resistivities will be erroneously high. Various algorithms and inversion techniques can be used to partially correct for the effects of permeability and permittivity.

Apparent resistivity maps portray all of the information for a given frequency over the entire survey area. This full coverage contrasts with the electromagnetic anomaly map, which provides information only over interpreted conductors. The large dynamic range afforded by the multiple frequencies makes the apparent resistivity parameter an excellent mapping tool.

The preliminary apparent resistivity maps and images were carefully inspected to identify any lines or line segments that might require base level adjustments. Subtle changes between in-flight calibrations of the system can result in line-to-line differences that are more recognizable in resistive (low signal amplitude) areas. If required, manual level adjustments were carried out to eliminate or minimize resistivity differences that can be attributed, in part, to changes in operating temperatures. These levelling adjustments were usually very subtle, and did not result in the degradation of discrete anomalies.

Dielectric Permittivity and Magnetic Permeability Corrections

In resistive areas having magnetic rocks, the magnetic and dielectric effects will both generally be present in high-frequency EM data, whereas only the magnetic effect will exist in low-frequency data (Huang and Fraser 2001). The magnetic permeability is first obtained from the EM data at the lowest frequency, because the ratio of the magnetic response to conductive response is maximized and because displacement currents are negligible. The homogeneous half-space model was used. The computed magnetic permeability was then used along with the in-phase and quadrature response at the highest frequency to obtain the relative dielectric permittivity, again using the homogeneous half-space model. The highest frequency was used because the ratio of dielectric response to conductive response is maximized. The resistivity was then determined from the measured in-phase and quadrature components of each frequency, given the relative magnetic permeability and relative dielectric permittivity.

Magnetic Field Processing

A fourth difference editing routine was applied to the magnetic data to remove any spikes. The aeromagnetic data were corrected for diurnal variation using the magnetic base station data. The results were then levelled using tie and traverse line intercepts after removing the IGRF on a survey data point/date basis. Manual adjustments were applied to any lines that required levelling, as indicated by shadowed images of the gridded magnetic data. The manually levelled data were then subjected to a microlevelling filter.

Digital Elevation

The radar altimeter values were subtracted from the differentially corrected and de-spiked GPS-Z data to produce profiles of the height above the ellipsoid along the survey lines. The calculated digital terrain data were then tie-line levelled and adjusted to mean sea level. Any remaining subtle line-to-line discrepancies were manually removed. After the manual corrections were applied, the digital terrain data were filtered with a microlevelling algorithm.

The accuracy of the elevation calculation is directly dependent on the accuracy of the 2 input parameters, ALTR and GPS-Z. The ALTR value may be erroneous in areas of heavy tree cover, where the altimeter reflects the distance to the tree canopy rather than the ground. The GPS-Z value is primarily dependent on the number of available satellites. Although post-processing of GPS data will yield X and Y accuracies in the order of 1 to 2 m, the accuracy of the Z value is usually much less, sometimes in the ± 10 m range. Further inaccuracies may be introduced during the interpolation and gridding process.

Radiometrics

All radiometric data reductions performed by Fugro rigorously follow the procedures described in the IAEA Technical Report 6. All processing of radiometric data was undertaken at the natural sampling rate of the spectrometer, i.e., one second. The data were not interpolated to match the fundamental 0.1 second interval of the EM and magnetic data.

The following sections describe each step in the process.

Pre-filtering

The radar altimeter data were processed with a 15-point median filter to remove spikes.

Reduction to Standard Temperature and Pressure

The radar altimeter data were converted to effective height (h_e) in feet using the acquired temperature and pressure data, according to the following formula:

$$h_e = h * \frac{273.15}{T + 273.15} * \frac{P}{1013.25}$$

where: h is the observed crystal to ground distance in feet
 T is the measured air temperature in degrees Celsius
 P is the barometric pressure in millibars

Live Time Correction

The spectrometer, an Exploranium GR-820, uses the notion of “live time” to express the relative period of time the instrument was able to register new pulses per sample interval. This is the opposite of the traditional “dead time”, which is an expression of the relative period of time the system was unable to register new pulses per sample interval. The GR-820 measures the live time electronically, and outputs the value in milliseconds. The live time correction is applied to the total count, potassium, uranium, thorium, upward uranium and cosmic channels. The formula used to apply the correction is as follows:

$$C_{lt} = C_{raw} * \frac{1000.0}{L}$$

where: C_{lt} is the live-time corrected channel in counts per second
 C_{raw} is the raw channel data in counts per second
 L is the live time in milliseconds

Intermediate Filtering

Two parameters were filtered, but not returned to the database:

Radar altimeter was smoothed with a 3-point Hanning filter (hef).

The Cosmic window was smoothed with a 3-point Hanning filter (Cosf).

Aircraft and Cosmic Background

Aircraft background and cosmic stripping corrections were applied to the total count, potassium, uranium, thorium and upward uranium channels using the following formula:

$$C_{ac} = C_{lt} - (a_c + b_c * Cos_f)$$

where: C_{ac} is the background and cosmic corrected channel

C_{lt} is the live time corrected channel

a_c is the aircraft background for this channel

b_c is the cosmic stripping coefficient for this channel

Cos_f is the filtered Cosmic channel

Radon Background

The determination of calibration constants that enable the stripping of the effects of atmospheric radon from the downward-looking detectors through the use of an upward-looking detector is divided into two parts:

1. Determine the relationship between the upward- and downward-looking detector count rates for radiation originating from the ground.
2. Determine the relationship between the upward- and downward-looking detector count rates for radiation due to atmospheric radon.

The procedures to determine these calibration factors are documented in International Atomic Energy Agency (IAEA) Report #323 on airborne gamma-ray surveying (IAEA 1991). The calibrations for the first part were determined as outlined in the report.

The latter case normally requires many over-water measurements where there is no contribution from the ground. Where this is not possible, it is standard procedure to establish a test line over which a series of repeat measurements are acquired. From these repeat flights, any change in the downward uranium window due to variations in radon background would be directly related to variations in the upward window and the other downward windows.

The validity of this technique rests on the assumption that the radiation from the ground is essentially constant from flight to flight. Inhomogeneities in the ground, coupled with deviations in the flight path between test runs, add to the inaccuracy of the accumulated results. Variations in flying heights and other environmental factors also contribute to the uncertainty.

The use of test lines is a common solution for a fixed-wing acquisition platform. The ability of rotary wing platforms to hover at a constant height over a fixed position eliminates a number of the variations that degrade the accuracy of the results required for this calibration.

A test site was established near the survey area. The tests were carried out at the start and end of each day. Data were acquired over a four-minute period at the nominal survey altitude of 60 m. The data were then corrected for live time, aircraft background and cosmic activity.

Once the survey was completed, the relationships between the counts in the downward uranium window and in the other four windows due to atmospheric radon were determined using linear regression for each of the hover sites. The following equations were used:

$$\begin{aligned}u_r &= a_u U_r + b_u \\K_r &= a_K U_r + b_K \\T_r &= a_T U_r + b_T \\I_r &= a_I U_r + b_I\end{aligned}$$

where: U_r is the radon component in the upward uranium window.
 K_r , U_r , T_r and I_r are the radon components in the various windows of the downward detectors.
the various “a” and “b” coefficients are the required calibration constants

In practice, only the “a” constants were used in the final processing. The “b” constants, which are normally near zero for over-water calibrations, were of no value as they reflected the local distribution of the ground concentrations measured in the five windows. The thorium, uranium and upward uranium data for each line were copied into temporary arrays and then smoothed with 21, 21 and 51 point Hanning filters to produce Th_f , U_f , and u_f respectively. The radon component in the downward uranium window was then determined using the following formula:

$$U_r = \frac{u_f - a_1 * U_f - a_2 * Th_f + a_2 * b_{Th} - b_u}{a_u - a_1 - a_2 * a_{Th}}$$

where: U_r is the radon component in the downward uranium window
 u_f is the filtered upward uranium
 U_f is the filtered uranium
 Th_f is the filtered thorium
 a_1 , a_2 , a_u and a_{Th} are proportionality factors and
 b_u and b_{Th} are constants determined experimentally

The effects of radon in the downward uranium are removed by simply subtracting U_r from U_{ac} . The effects of radon in the total count, potassium, thorium and upward uranium are then removed based upon previously established relationships with U_r . The corrections are applied using the following formula:

$$C_{rc} = C_{ac} - (a_c * U_r + b_c)$$

where: C_{rc} is the radon corrected channel
 C_{ac} is the background and cosmic corrected channel
 U_r is the radon component in the downward uranium window
 a_c is the proportionality factor and
 b_c is the constant determined experimentally for this channel

Compton Stripping

Following the radon correction, the potassium, uranium and thorium were corrected for spectral overlap. First, α , β and γ the stripping ratios, were modified according to altitude. Then an adjustment factor based on a , the reversed stripping ratio, uranium into thorium, is calculated. (Note: the stripping ratio altitude correction constants are expressed in change per metre. A constant of 0.3048 is required to conform to the internal usage of height in feet):

$$\alpha_h = \alpha - (h_{ef} * 0.00049)$$

$$\alpha_r = \frac{1.0}{1.0 + a * \alpha_h}$$

$$\beta_h = \beta - (h_{ef} * 0.00065)$$

$$\gamma_h = \gamma - (h_{ef} * 0.00069)$$

where: α , β , γ are the Compton stripping coefficients
 α_h , β_h , γ_h are the height corrected Compton stripping coefficients
 h_{ef} is the height above ground in metres
 α_r is the scaling factor correcting for back scatter
 a is the reverse stripping ratio

The stripping corrections were then carried out using the following formulae:

$$Th_h = (Th_{rc} - a * U_{rc}) * \alpha_r$$

$$K_c = K_{rc} - \gamma_h * U_c - \beta_h * Th_c$$

$$U_c = (U_{rc} * -\alpha_h * Th_{rc}) * \alpha_r$$

where: U_c , Th_c and K_c are corrected uranium, thorium and potassium
 $\alpha_h, \beta_h, \gamma_h$ are the height corrected Compton stripping coefficients
 U_{rc} , Th_{rc} and K_{rc} are radon-corrected uranium, thorium and potassium
 α_r is the backscatter correction

Attenuation Corrections

The total count, potassium, uranium and thorium data were then corrected to a nominal survey altitude, in this case 200 feet. This was done according to the equation:

$$C_a = C * e^{\mu(h_{ef} - h_0)}$$

where: C_a is the output altitude corrected channel

C is the input channel

e^{μ} is the attenuation correction for that channel

h_{ef} is the effective altitude in feet

h_0 is the nominal survey altitude to correct to 200 feet

5. FINAL DATA COMPILATION AND PROCESSING

Base Maps

Base maps of the survey area were supplied by the Ontario Ministry of Northern Development and Mines.

Projection Description

Datum:	NAD83 (Canada)
Ellipsoid:	GRS80
Projection:	UTM Zone 17N (CM=81° W)
False Northing:	0 m
False Easting:	500 000 m
Scale factor:	0.9996

Magnetic Microlevelling

Microlevelling is the process of removing residual flight line noise that remains after conventional levelling using control lines. It has become increasingly important as the resolution of aeromagnetic surveys has improved and the requirement of interpreting subtle geophysical anomalies has increased.

To isolate and remove this noise, the following procedure was employed. An elliptical reject filter, aligned with the flight lines, was first applied to the levelled total magnetic field grid. This filter removes features with a long wavelength in the flight line direction, but a short wavelength in the transverse direction. While removing the unwanted residual levelling errors, it also significantly distorts higher amplitude anomalies.

In order to minimize the effect on real anomalies, the flight path was “threaded” through the filtered grid and a database profile channel was created from the grid. The difference between the control line levelled magnetic profile and this filtered profile was calculated. The difference profile was clipped to the amplitude of the observed noise in the grid and a half cosine roll-off filter was then applied to this channel and a final correction profile was derived. For most of the survey area, the correction was limited to an amplitude of +/- 5nT, with wavelengths longer than 1 km. In the area of 37.5 m spaced infill lines, however, altitude and horizontal position errors were still apparent. In the area of the infill, the correction profile was allowed to reach ±25 nT, with wavelengths as short as 100 m. The microlevel correction profile was applied to the levelled magnetic profile and a final magnetic profile channel was created.

GSC Levelling

The final step in the magnetic profile processing was to level the data set to the 200 m Ontario Master grid (OGS 1999), which has been compiled and levelled to the 812.8 m magnetic datum

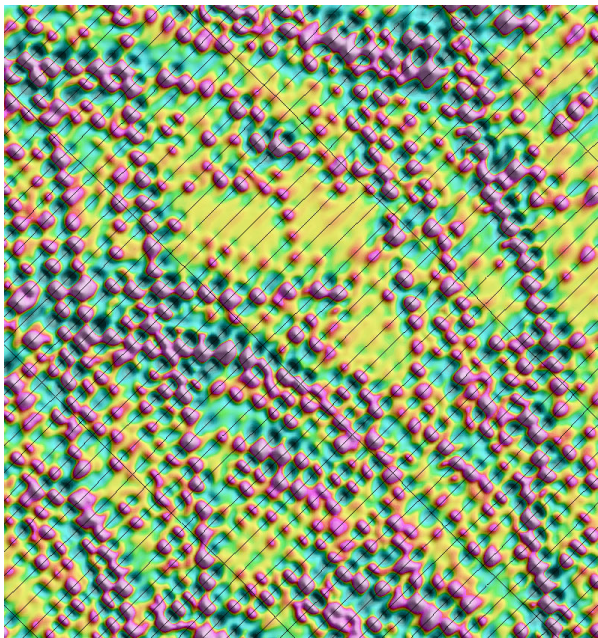
from the Geological Survey of Canada (GSC). The levelling process must retain all the detail of the newer low-altitude survey and only make corrections on the order of 10 km or more. To accomplish this, a variation on a method developed by Patterson, Grant and Watson (Reford et al. 1990) was used. The procedure follows:

The final total magnetic data were gridded at a 200 m cell size and upward continued to a height of 305 m, to match the nominal terrain clearance of the Ontario master grid. The difference between the upward continued grid and the Ontario master grid was calculated. An FFT 2-D low-pass filter was applied to a grid of the difference, which retained wavelengths longer than 10 km. This filtered grid was re-gridded at a 20 m cell size and the flight path was threaded through the grid to create a correction profile. This long wavelength correction profile was subtracted from the final magnetic channel to great a GSC-levelled (mag_gsclevel) channel.

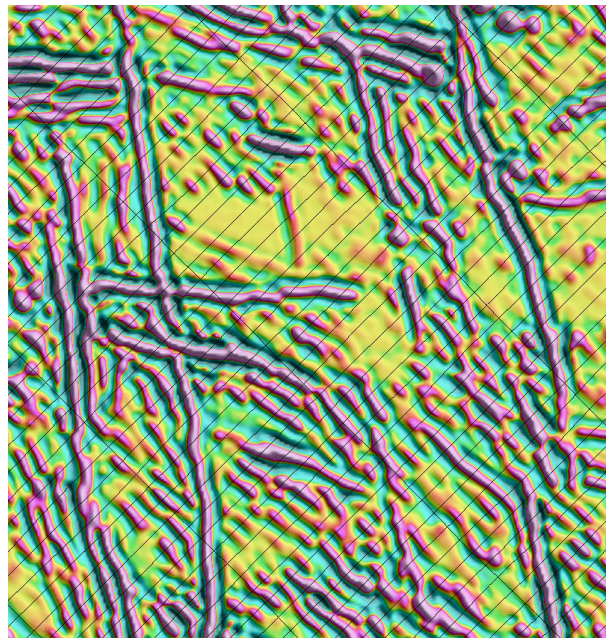
Strike-Interpretive Gridding

The GSC-levelled magnetic data were preliminarily gridded, using a minimum curvature algorithm and significant beading or boudinage was noted in the grid. These aliasing and gridding artefacts are greatly exaggerated by subsequent processing methods, such as second vertical derivative. Scott Hogg & Associates Ltd. has developed a strike-interpretive gridding routine (SI-Grid) where the interpolation between flight lines can be manually driven to protect trends that vary throughout the map.

In the figure below there are 2 presentations of an area within the data set. On the left is a second vertical derivative of the minimum curvature grid. On the right is the SI-Grid version.



2VG – Minimum Curvature



2VG – SI- Grid

The GSC-levelled data were gridded using the SI-Grid routine. Both the minimum curvature grid and the SI-Grid versions of the magnetic data are included with the dataset.

Second Vertical Derivative Grid

The second vertical derivative of the total magnetic field SI-Grid was computed to enhance small and weak near-surface anomalies and as an aid to delineate the contacts of the lithologies having contrasting susceptibilities. The location of contacts or boundaries is usually traced by the zero contour of the second vertical derivative map.

The calculation was done in the frequency domain by combining the transfer function of the second vertical derivative and a half cosine roll-off filter with an 80 m cut-off wavelength.

Keating Correlation Coefficients

Possible kimberlite targets are identified from the residual magnetic intensity data, based on the identification of roughly circular anomalies. This procedure is automated by using a known pattern recognition technique (Keating 1995), which consists of computing, over a moving window, a first-order regression between a vertical cylinder model anomaly and the gridded magnetic data. Only the results where the absolute value of the correlation coefficient is above a threshold of 75% were retained. On the magnetic maps, the results are depicted as circular symbols, scaled to reflect the correlation value. The most favourable targets are those that exhibit a cluster of high amplitude solutions. Correlation coefficients with a negative value correspond to reversely magnetised sources.

The cylinder model parameters are as follows:

- Cylinder diameter: 200 m
- Cylinder length: infinite
- Overburden thickness: 3 m
- Magnetic inclination: 73.7°N
- Magnetic declination: 9.8°W
- Magnetization scale factor: 100
- Model window size: 10 by 10 cells (400 by 400 m)
- Model window grid cell size: 40 m

It is important to be aware that other magnetic sources may correlate well with the vertical cylinder model, whereas some kimberlite pipes of irregular geometry may not. The user should study the magnetic anomaly that corresponds with the Keating symbols, to determine whether it does resemble a kimberlite pipe signature, reflects some other type of source or even noise in the data, e.g., boudinage (beading) effect of the bi-cubic spline gridding. All available geological information should be incorporated in kimberlite pipe target selection.

Apparent Resistivity Grids

The contractor-provided channels of apparent resistivity were gridded using a bi-cubic spline algorithm. To reduce a lot of noted ringing and between-line artefacts, values in the grid that

were outside the range of the input profile data were deleted. The missing values were filled in and five passes of a 3 by 3 Hanning filter were applied. Final grids of apparent resistivity are included for the following frequencies:

900 Hz
1000 Hz
7200 Hz
56 kHz

Radiometric Grids

To supplement the contractor-provided radiometric data, a profile channel of the ratio of potassium over thorium was created. To avoid division by zero (or near-zero) artefacts, the thorium data were clipped at a minimum of 1 cps prior to the calculation. The following data were gridded using a bi-cubic spline algorithm:

Total count
Potassium
Uranium
Thorium
Potassium/Thorium

Negative values in the grids, introduced by either the radiometric processing or the gridding algorithm were removed and the missing data interpolated. Finally, a 7 by 7 Hanning convolution filter was applied to each grid.

Ternary Image

A ternary map image map was created, using the final radiometric grids. A Red, Green, Blue, Intensity (RGBI) scheme was used.

To better display the relative concentrations, the grids were sum-normalised using the formulae:

$$K_{norm} = \frac{K}{K + U + Th}$$

$$U_{norm} = \frac{U}{K + U + Th}$$

$$Th_{norm} = \frac{Th}{K + U + Th}$$

The denominator of the normalization factor (K + U + Th) was limited to values greater than 1.

The RGBI colouring used the following colour transforms:

Red (R): K_{norm} (cps), data limits of 0 to 1, equal area histogram
Green (G): U_{norm} (cps), data limits of 0 to 1, equal area histogram
Blue (B): T_{norm} (cps), data limits of 0 to 1, equal area histogram
Intensity (I): total count (cps), data limits of 99% of data values, logarithmic

Electromagnetic Anomaly Symbols

The electromagnetic anomalies organized into classes, based on the calculated conductance. The table below shows the symbols used for each conductance range.

LEGEND

ELECTROMAGNETIC ANOMALY SYMBOLS

Anomaly	Conductance Classification
●	> 5.0 siemens
◐	1.7 - 4.9 siemens
◑	1.0 - 1.6 siemens
◒	0.6 - 0.9 siemens
⊕	0.2 - 0.5 siemens
○	0.0 - 0.1 siemens
*	surficial conductor
⊞	cultural response

6. FINAL PRODUCTS

The following products are included in the compilation:

Map products at 1:20 000

- Colour residual magnetic field grid (trend enhanced) with contours and flightlines, plotted on a planimetric base
- Shaded colour image of the second vertical derivative of the magnetics (trend enhanced) and Keating kimberlite coefficient anomalies on a planimetric base
- Ternary RGBI radioelement image, with flightlines and thumbnail images of K, U, Th and TC on a planimetric base
- Colour apparent resistivity (at 7200 Hz) grid with contours and flightlines, plotted on a planimetric base

Profile databases

- Database with EM, radiometric and magnetic data sampled at 10 samples per second in both Geosoft® GDB and ASCII format.
- Raw full - spectrum radiometric data sampled at 1 sample/sec in both Geosoft® GDB and ASCII format.

EM anomaly databases

- EM anomaly databases in both Geosoft® GDB and ASCII CSV format

Kimberlite coefficient database

- Keating kimberlite coefficient anomaly databases in both Geosoft® GDB and ASCII CSV format.

Data grids

Data grids, in both Geosoft® GRD and GXF formats, gridded from co-ordinates in UTM Zone 17N, NAD83 datum, of the following parameters:

- GSC-levelled magnetic field (normal and strike-interpretive)
- Second vertical derivative of the GSC-levelled magnetic field (normal and strike-interpretive)
- Digital elevation model
- Total count
- Potassium
- Thorium
- Uranium
- Potassium / thorium ratio

- EM resistivity 900 Hz
- EM resistivity 1000 Hz
- EM resistivity 7200 Hz
- EM resistivity 56 kHz

GeoTIFF images:

- Colour residual magnetic field grid plotted on a planimetric base
- Shaded colour image of the second vertical derivative of the magnetic grid and Keating kimberlite coefficient anomalies on a planimetric base
- Total count grid on a planimetric base
- Potassium grid on a planimetric base
- Uranium on a planimetric base
- Thorium on a planimetric base
- Potassium / thorium on a planimetric base
- RGBI ternary image of K / eTh / eU and TC
- EM resistivity 900 Hz on a planimetric base
- EM resistivity 1000 Hz on a planimetric base
- EM resistivity 7200 Hz on a planimetric base
- EM resistivity 56 kHz on a planimetric base

DXF vector files

- Flight path
- Keating kimberlite coefficient anomalies
- Electromagnetic anomaly symbols
- Residual magnetic field contours
- EM resistivity 7200 Hz contours

Project report

- Provided as Microsoft® Word (.doc) and portable document format (.pdf) files.

REFERENCES

- Fugro Airborne Surveys Corp. 2008. Operations DIGHEM Survey for Augen Gold Corp. Gogama Project Ontario; unpublished report for Augen Gold Corp.
- Huang, H. and Fraser, D.C. 2001. Mapping of the resistivity, susceptibility, and permittivity of the earth using a helicopter-borne electromagnetic system; *Geophysics*, v.66, p.148-157.
- International Atomic Energy Agency 1991. Airborne gamma-ray spectrometer surveying; International Atomic Energy Agency, Technical Report Series No. 323.
- Keating, P.B. 1995. A simple technique to identify magnetic anomalies due to kimberlite pipes; *Exploration and Mining Geology*, v.4, no.2, p.121-125.
- Ontario Geological Survey 1999. Single master gravity and aeromagnetic data for Ontario; Ontario Geological Survey, Geophysical Data Set 1036.
- Reford, S.W., Gupta, V.K., Paterson, N.R., Kwan, K.C.H., and Macleod, I.N. 1990. Ontario master aeromagnetic grid: A blueprint for detailed compilation of magnetic data on a regional scale; *in* Expanded Abstracts, Society of Exploration Geophysicists, 60th Annual International Meeting, San Francisco, v.1, p.617-619.

APPENDIX A GENERAL ARCHIVE DEFINITION

Survey 1238 was carried out using Fugro Airborne Survey's electromagnetic DIGHEM system with magnetometer and gamma-ray spectrometer.

Data File Layout

The files for the Opeepeesway Lake Geophysical Survey 1238 are archived on a single DVD. The content of the ASCII and Geosoft® binary file types are identical. They are provided in both forms to suit the user's available software. The survey data are divided as follows:

- ASCII (GXF) grids
 - total (residual) field magnetics (minimum curvature)
 - total (residual) field magnetics (trend enhanced)
 - second vertical derivative of the total field magnetics (minimum curvature)
 - second vertical derivative of the total field magnetics (trend enhanced)
 - apparent resistivity 900 Hz
 - apparent resistivity 1000 Hz
 - apparent resistivity 7200 Hz
 - apparent resistivity 56 kHz
 - total count spectrometer
 - potassium
 - uranium
 - thorium
 - potassium / thorium ratio
- Keating correlation (kimberlite) database (ASCII CSV format)
- EM anomaly database (ASCII CSV format)
- DXF files:
 - flight path
 - Keating correlation (kimberlite) anomalies
 - EM anomalies
 - total field magnetic contours
 - EM resistivity 7200 Hz contours
- GEOTIFF images
 - colour total field magnetics with base map
 - colour shaded relief of second vertical derivative with base map and Keating correlation symbols
 - colour resistivity 900 Hz with basemap
 - colour resistivity 1000 Hz with basemap
 - colour resistivity 7200 Hz with basemap

- colour resistivity 56 kHz with basemap
- colour total count with basemap
- colour potassium with basemap
- colour uranium with basemap
- colour thorium with basemap
- colour potassium/thorium ratio with basemap
- radiometric ternary image with basemap

- Geosoft® Binary (GRD) grids
 - total (residual) field magnetics (minimum curvature)
 - total (residual) field magnetics (trend enhanced)
 - second vertical derivative of the total field magnetics (minimum curvature)
 - second vertical derivative of the total field magnetics (trend enhanced)
 - apparent resistivity 900 Hz
 - apparent resistivity 1000 Hz
 - apparent resistivity 7200 Hz
 - apparent resistivity 56 kHz
 - total count spectrometer
 - potassium
 - uranium
 - thorium
 - potassium/thorium ratio

- Keating correlation (kimberlite) database (Geosoft® GDB format)

- EM anomaly database (Geosoft® GDB format)

- ASCII Profile data
 - Profile database of spectrometry, electromagnetic and magnetic data (10 Hz sampling) in ASCII (XYZ) format
 - Profile database of raw 256 channel radiometric spectrum data (1 Hz sampling) in ASCII (XYZ) format

- Binary Profile data
 - Profile database of spectrometry, electromagnetic and magnetic data (10 Hz sampling) in Geosoft® GDB format
 - Profile database of raw 256 channel radiometric spectrum data (1 Hz sampling) in Geosoft® GDB format

- Survey report (Microsoft® Word (.doc) and portable document format (.pdf) files).

Coordinate Systems

The profile and anomaly data include two coordinate systems:

- Universal Transverse Mercator (UTM) projection, Zone 17N, NAD83 datum, Canada local datum
- Latitude/longitude coordinates, NAD83 datum, Canada local datum

The gridded data are provided in one UTM coordinate system:

- Universal Transverse Mercator (UTM) projection, Zone 17N, NAD83 datum, Canada local datum

Profile Data

The profile data are provided in 2 formats, 1 ASCII and 1 binary:

ASCII

Opeepeesway.xyz ASCII file of spectrometry, electromagnetic and magnetic data, at 10 Hz
OLspec256.xyz ASCII file of raw 256 channel radiometric spectrum data at 1 Hz

Binary

Opeepeesway.gdb Geosoft® OASIS Montaj™ binary database file (no compression) of spectrometry electromagnetic and magnetic data, sampled at 10 Hz
Alspect256.gdb Geosoft® OASIS Montaj™ binary database file (no compression) of raw 256 channel radiometric spectrum data, sampled at 1 Hz

APPENDIX B PROFILE ARCHIVE DEFINITION

The line profile databases opeepeesway.xyz/gdb (both file types contain the same set of data channels) are summarised as follows:

Channel Name	Description	Units
x_nad83	easting in UTM co-ordinates using NAD83 datum	metres
y_nad83	northing in UTM co-ordinates using NAD83 datum	metres
lon_nad83	longitude using NAD83 datum	decimal-degrees
lat_nad83	latitude using NAD83 datum	decimal-degrees
gps_z_final	differentially corrected GPS Z (NAD83 datum)	metres above sea level
fiducial	fiducial	seconds
flight	flight number	
line	flightline number	
radar_final	corrected radar altimeter	metres above terrain
dem	digital elevation model	metres ASL
height_mag	magnetometer height	metres above terrain
mag_diurn	diurnally-corrected magnetic field	nanoteslas
mag_igrf	IGRF-corrected magnetic field	nanoteslas
mag_lev	levelled magnetic field	nanoteslas
mag_final	micro-levelled magnetic field	nanoteslas
mag_gsclevel	GSC-levelled magnetic field	nanoteslas
height_em	electromagnetic receiver height	metres above terrain
cpi_900_final	levelled coplanar inphase at 900 Hz	parts per million
cpq_900_final	levelled coplanar quadrature at 900 Hz	parts per million
cxi_1000_final	levelled coaxial inphase at 1000 Hz	parts per million
cxq_1000_final	levelled coaxial quadrature at 1000 Hz	parts per million
cxi_5500_final	levelled coaxial inphase at 5500 Hz	parts per million
cxq_5500_final	levelled coaxial quadrature at 5500 Hz	parts per million
cpi_7200_final	levelled coplanar inphase at 7200 Hz	parts per million
cpq_7200_final	levelled coplanar quadrature at 7200 Hz	parts per million
cpi_56K_final	levelled coplanar inphase at 56000 Hz	parts per million
cpq_56K_final	levelled coplanar quadrature at 56000 Hz	parts per million
power	60 frequency power line monitor	millivolts
ares_900	apparent resistivity for coplanar coil pair – 900 Hz	ohm-metres
ares_1000	apparent resistivity for coaxial coil pair – 1000 Hz	ohm-metres
ares_7200	apparent resistivity for coplanar coil pair – 7200 Hz	ohm-metres
ares_56K	apparent resistivity for coplanar coil pair – 56K Hz	ohm-metres
depth_900	EM anomaly depth for coplanar coil pair – 900 Hz	metres below surface
depth_1000	EM anomaly depth for coaxial coil pair – 1000 Hz	metres below surface
depth_7200	EM anomaly depth for coplanar coil pair – 7200 Hz	metres below surface
depth_56K	EM anomaly depth for coplanar coil pair – 56K Hz	metres below surface
live_time	gamma-ray spectrometer live time	milliseconds
cosmic	cosmic window	counts per second
radon	upward-looking uranium window	counts per second
total_count_win	windowed total count	counts per second
potassium_win	windowed potassium	counts per second
uranium_win	windowed uranium	counts per second
thorium_win	windowed thorium	counts per second
k_over_th	ratio of potassium over thorium	
air_temp	outside air temperature	degrees Celsius
pressure	outside air pressure	kPa
effective_ht	effective height (spectrometer)	metres above terrain

The line profile databases olspec256.xyz/gdb (both file types contain the same set of data channels) are summarised as follows:

<u>Channel Name</u>	<u>Description</u>	<u>Units</u>
x_nad83	easting in UTM co-ordinates, NAD83 zone 15N	metres
y_nad83	northing in UTM co-ordinates, NAD83 zone 15N	metres
long_nad83	longitude, NAD83 datum	decimal-degrees
lat_nad83	latitude, NAD83 datum	decimal-degrees
fiducial	Fiducial	seconds
line	database line number	
spc_rawd83	raw downward looking 256 channel gamma-ray spectrum	counts per second

APPENDIX C ANOMALY ARCHIVE DEFINITION

Electromagnetic Anomaly Data

The electromagnetic anomaly data are provided in two formats, one ASCII and one binary:

Both file types contain the same set of data channels, summarized as follows:

Channel Name	Description	Units
x_nad83	easting in UTM co-ordinates using NAD83 datum	metres
y_nad83	northing in UTM co-ordinates using NAD83 datum	metres
lon_nad83	longitude using NAD83 datum	decimal-degrees
lat_nad83	latitude using NAD83 datum	decimal-degrees
dem	digital elevation model	metres ASL
line	flightline number	
fiducial	fiducial	
flight	flight number	
cpi_900_final	levelled coplanar inphase at 900 Hz	ppm
cpq_900_final	levelled coplanar quadrature at 900 Hz	ppm
cxi_1000_final	levelled coaxial inphase at 1000 Hz	ppm
cxq_1000_final	levelled coaxial quadrature at 1000 Hz	ppm
cxi_5500_final	levelled coaxial inphase at 5500 Hz	ppm
cxq_5500_final	levelled coaxial quadrature at 5500 Hz	ppm
cpi_7200_final	levelled coplanar inphase at 7200 Hz	ppm
cpq_7200_final	levelled coplanar quadrature at 7200 Hz	ppm
cpi_56K_final	levelled coplanar inphase at 56000 Hz	ppm
cpq_56K_final	levelled coplanar quadrature at 56000 Hz	ppm
ares_900	apparent resistivity for coplanar coil pair – 900 Hz	ohm-metres
ares_1000	apparent resistivity for coaxial coil pair – 1000 Hz	ohm-metres
ares_7200	apparent resistivity for coplanar coil pair – 7200 Hz	ohm-metres
ares_56K	apparent resistivity for coplanar coil pair – 56K Hz	ohm-metres
height_em	electromagnetic receiver height	metres above terrain
anomaly_no	nth anomaly along the survey line	
anomaly_id	unique anomaly identifier	
anomaly_type	anomaly classification	
mag_correlation	magnetic correlation	nanoteslas
vert_sheet_conductance	conductance of vertical plate model (5500 Hz)	siemens
vert_sheet_depth	depth of vertical plate model (5500 Hz)	metres
heading	direction of flight	degrees
survey_number	survey number	

The unique anomaly identifier (anomaly_id) is a ten digit integer in the format 1LLLLLLAAA where 'LLLLLL' holds the line number (and leading zeroes pad short line numbers to six digits). The 'AAA' represents the numeric anomaly identifier (anomaly_no) for that line padded with leading zeroes to three digits. The leading 1 indicates that the anomaly was identified as likely having a normal or surficial source. For example, 1000101007 represents the seventh anomaly on Line 101. Anomalies identified as likely having a cultural source do not include the leading 1, and take the format LLLLLLAAA. For example, 101007 represents the seventh cultural anomaly on Line 101. When combined with the survey number (survey_no), the anomaly identifier provides an electromagnetic anomaly number unique to all surveys archived by the Ontario Geological Survey.

APPENDIX D KEATING CORRELATION ARCHIVE DEFINITION

Kimberlite Pipe Correlation Coefficients

The Keating kimberlite pipe correlation coefficient data are provided in two formats; ASCII and binary.

Both file types contain the same set of data channels, summarized as follows:

Channel Name	Description	Units
x_nad83	UTM easting - NAD83, zone 17N	metres
y_nad83	UTM northing - NAD83, zone 17N	metres
lon_nad83	longitude using NAD83 datum	decimal-degrees
lat_nad83	latitude using NAD83 datum	decimal-degrees
corr_coeff	correlation coefficient	percent x 10
pos_coeff	positive correlation coefficient	percent
neg_coeff	negative correlation coefficient	percent
norm_error	standard error normalized to amplitude	percent
amplitude	peak-to-peak anomaly amplitude within window	nanoteslas

APPENDIX E GRID ARCHIVE DEFINITION

Gridded Data

The gridded data are provided in two formats, one ASCII (.gxf) and one binary (.grd)

The grids are summarized as follows:

All grids are NAD83 UTM Zone 17N, with a grid cell size of 20 by 20 m.

OLMAG83.grd/.gxf	– GSC-levelled residual magnetic intensity
OLMAGT83.grd/.gxf	– GSC-levelled residual magnetic intensity (trend enhanced)
OL2VD83.grd/.gxf	– Second vertical derivative of residual magnetic intensity
OL2VDT83.grd/.gxf	– Second vertical derivative of residual magnetic intensity (trend enhanced)
OLDEM83.grd/.gxf	– Digital elevation model
OLTC83.grd/.gxf	– Radiometric total count
OLK83.grd/.gxf	– Potassium
OLU83.grd/.gxf	– Uranium
OLTH83.grd/.gxf	– Thorium
OLK_over_TH83	– Potassium over thorium ratio
OL900RES83.grd/.gxf	– EM apparent resistivity 900 Hz
OL1000RES83.grd/.gxf	– EM apparent resistivity 1000 Hz
OL7200RES83.grd/.gxf	– EM apparent resistivity 7200 Hz
OL56KRES83.grd/.gxf	– EM apparent resistivity 56 kHz

APPENDIX F GEOTIFF AND VECTOR ARCHIVE DEFINITION

GeoTIFF Images

Geographically referenced colour images, incorporating a base map, are provided in GeoTIFF format for use in GIS applications:

OLMAG83.TIF	– GSC-levelled residual magnetic intensity (trend enhanced)
OL2VD83.TIF	– Second vertical derivative of GSC-levelled residual magnetic Intensity (trend enhanced) with Keating coefficient symbols
OLTC83.TIF	– Total Count
OLK83.TIF	– Potassium
OLU83.TIF	– Uranium
OLTH83.TIF	– Thorium
OLK_over_TH83.TIF	– Potassium over Thorium
OLTERN83.TIF	– Potassium, uranium, thorium, total count ternary image
OL900RES83.TIF	– Apparent resistivity 900 Hz
OL1000RES83.TIF	– Apparent resistivity 1000 Hz
OL7200RES83.TIF	– Apparent resistivity 7200 Hz
OL56KRES83.TIF	– Apparent resistivity 56 kHz

Vector Archives

Vector line work from the maps is provided in DXF ASCII format using the following naming convention:

OLPATH83.DXF	– Flight path of the survey area
OLKC83.DXF	– Keating correlation targets
OLANOM83.DXF	– Electromagnetic anomalies
OLMAGT83.DXF	– Contours of the residual magnetic (trend enhanced) intensity
OL7200RES83.DXF	– Contours of VLF-EM vertical component